Case history of the response of a longwall entry subjected to concentrated horizontal stress

C. Mark[a,*], W. Gale[b], D. Oyler[a], J. Chen[c]

[a]NIOSH, Rock Safety Engineering Branch, Pittsburgh Research Laboratory, P.O. Box 18070, Pittsburgh, PA 15236, USA
[b]Strata Control Technologies, Wollongong, NSW, Australia
[c]RAG Pennsylvania, Waynesburg, PA, USA

Abstract

The National Institute for Occupational Safety and Health (NIOSH) Pittsburgh Research Laboratory (PRL), RAG Pennsylvania and Strata Control Technologies of Australia collaborated in an intensive study of ground behavior, reinforcement performance, and stress redistribution at the Emerald Mine in Southwestern Pennsylvania. The study site was a longwall tailgate subjected to a severe horizontal stress concentration. Field measurements indicated that the stresses applied to the study site nearly doubled during longwall mining, resulting in roof deformations extending to a height of 4.8 m (16 ft) above the entry. A computer simulation of the field site was conducted using FLAC-2D, incorporating a broad range of rock behaviors and failure mechanisms. Comparison between the measurements and the simulation showed that the model was able to capture the most significant aspects of the roof and support system behavior, particularly, the extensive slip along bedding that created a partially destressed "softened" zone in the immediate roof. The model also showed that supplementing the normal roof bolt support pattern with cable bolts would allow the entry to survive a further 20–25% increase in the applied horizontal stress. Such information could have very practical application to the design of roof support systems for coal mines.

1. Introduction

Nearly 1500 roof falls occur each year in US underground coal mines, creating serious safety hazards and operational impacts. The cost of the support installed to prevent roof falls approaches $1 billion annually. Despite more than 50 years of research, no roof support design methodology has gained wide acceptance [1].

During the past 25 years, it has become evident that horizontal stresses are a significant contributing factor in many of the roof falls that occur underground [2]. An important breakthrough was the recognition that the stresses observed in mines are caused by global plate-tectonic forces [3]. Stress measurements have confirmed that the horizontal stress is typically two to three times the vertical in mines in the eastern US. Moreover, the longwall mining process can concentrate the horizontal stresses in specific, critical locations [4,5].

Stress concentrations that affect longwall gate entries are of particular concern (Fig. 1). These develop because the stress cannot be transmitted through the caved gob areas behind the longwall. Roof falls in either the tailgate or headgate are major safety hazards because they can disrupt ventilation or block vital travelways. They can also cause expensive production interruptions.

Most horizontal stress concentrations can be avoided through proper longwall panel orientation and sequencing. In some instances, however, the geometry of the reserve or some other consideration may limit mine planning options. For example, where one longwall panel is significantly longer than an adjacent, previously mined, panel, the resulting "stress window" can be very difficult to control (Fig. 2). Under these circumstances, the mine must prepare for severe ground conditions.

In the US, a common response to poor ground conditions is to install supplemental supports, such as

*Corresponding author. Tel.: +1 412 386 6522; fax: +1 412 386 6891.
E-mail address: cmark@cdc.gov (C. Mark).

cable bolts. The interaction between supplemental supports and primary roof bolts has received relatively little research attention, however [6]. The traditional way to study roof support performance has been with field measurements. During the 1990s, measurements of roof deformation and roof bolt load were made at a number of sites in the US [7,8]. These studies provided numerous insights into factors that effect bolt performance, including installed tension, bolt capacity, and grout annulus. Unfortunately, none of these studies was combined with stress measurements, or with extensive geologic characterization and rock mechanics testing. Moreover, sophisticated numerical modeling like that employed in some other countries has had relatively limited application to mining ground control in the US [9–11].

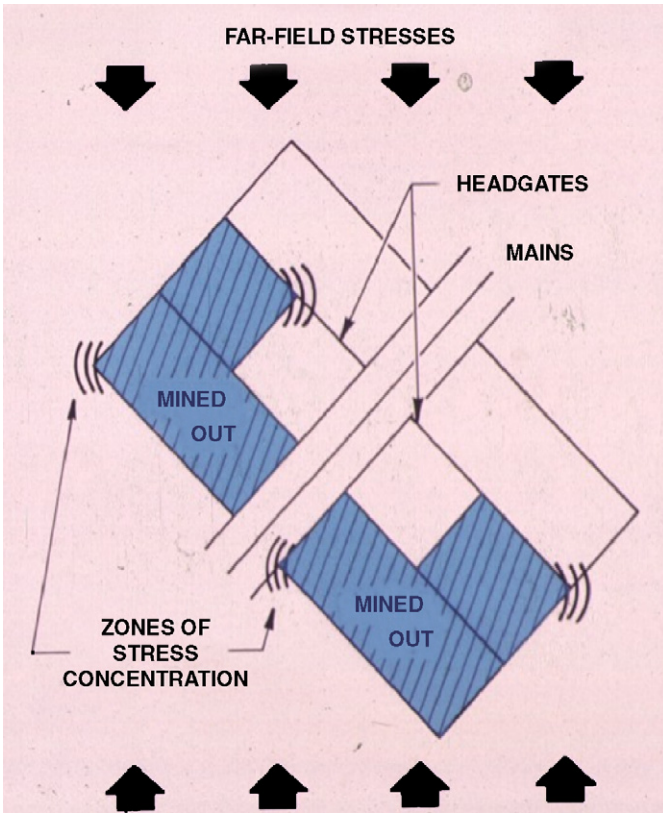

Fig. 1. Concentrations of horizontal stress caused by longwall panel extraction.

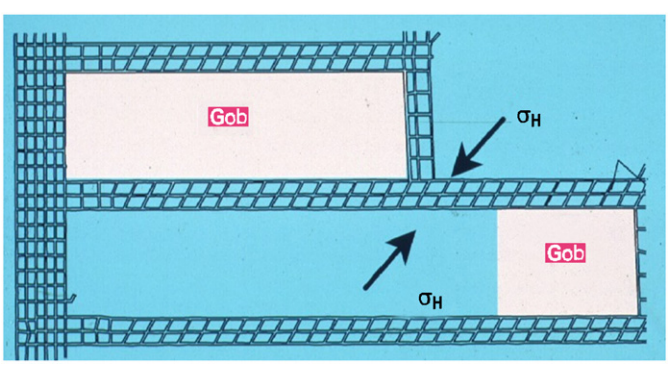

Fig. 2. A "stress window" created when horizontal stress is funneled between a pre-existing gob area and an approaching longwall panel.

The study described in this paper was the result of a collaboration between the National Institute for Occupational Safety and Health (NIOSH), RAG Pennsylvania (now Foundation Coal) and SCT Operations of Australia. Its goals were to:

- measure the stress changes and ground deformations resulting from an anticipated longwall stress concentration;
- evaluate the performance of typical US primary supports (roof bolts) in response to high horizontal stress;
- investigate the interaction between supplemental support systems (cable bolts) and primary supports; and
- refine the numerical modeling techniques required for analyzing support alternatives for high stress coal mine applications.

2. Study site

The site of the study was the tailgate of the 11 North longwall at the Emerald mine, located in Greene County, Pennsylvania (Fig. 3). The site was chosen because it was anticipated that the extension of 11 North beyond the start line of 10 North would result in a significant horizontal stress concentration [5]. From past experience at Emerald Mine, a horizontal stress window like the one created by 11 North could be expected to cause severe loading to be applied to the crosscut and tailgate entry. The location thus provided a rare opportunity to study the roof failure process as the applied horizontal stress increased during the progression from development through longwall mining.

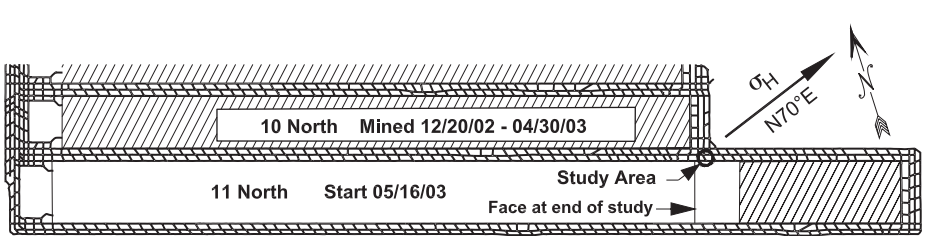

Fig. 3. Emerald mine and study site.

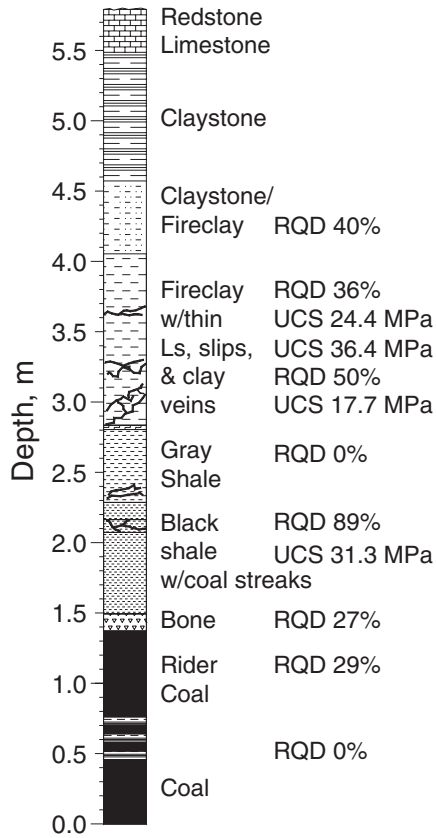

Fig. 4. Composite core log from the study site, showing rock physical properties. Data from the vertical corehole drilled in the study crosscut and from a surface corehole.

The Emerald Mine operates in the Pittsburgh coal bed in Southwest Pennsylvania, cutting roadways approximately 2.1–2.4 m (7–8 ft) high and 4.9 m (16 ft) wide. Approximately 0.3 m (1 ft) of roof shale is cut from the roof of the roadways. A geologic column of the mine roof obtained from a vertical core hole drilled at the site is shown in Fig. 4. The roof may be roughly divided into three units:

- a sequence of coals and weak, slickensided shales in the lowest 2.7 m (9 ft);
- a slightly stronger claystone sequence from 2.7 to 5.4 m (9–18 ft); and
- a significantly stronger limestone above 5.4 m (18 ft).

The in-mine coreholes barely reached the limestone, so its thickness and strength were estimated from a nearby surface corehole. The low uniaxial compressive strength and RQD for the bolted horizon results in an estimated coal mine roof rating (CMRR) of 37 [12].

Rock properties for the models were obtained from a combination of previous testing at the mine and from tests of underground core samples obtained from the study site. Of particular importance were angled core that were drilled at the study site and subjected to multi-stage triaxial testing[1] in order to determine bedding plane strength. The bedding plane strength test results are presented in Fig. 5 for the two shale units. The UCS profile and bedding cohesion profile used in the model is presented together with the laboratory core test results in Figs. 6 and 7,

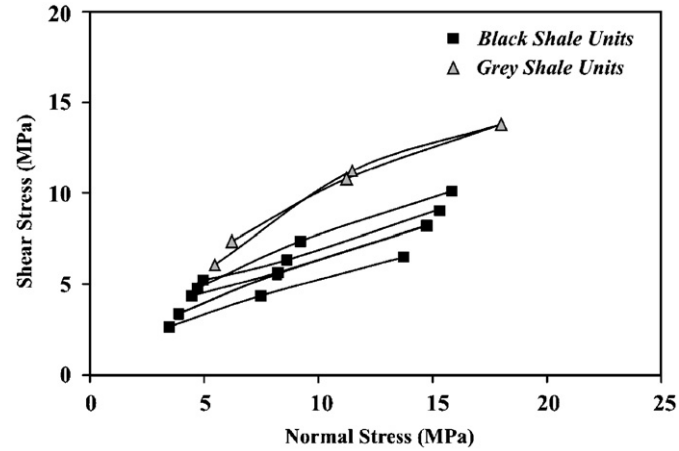

Fig. 5. Bedding plane test results from angled core.

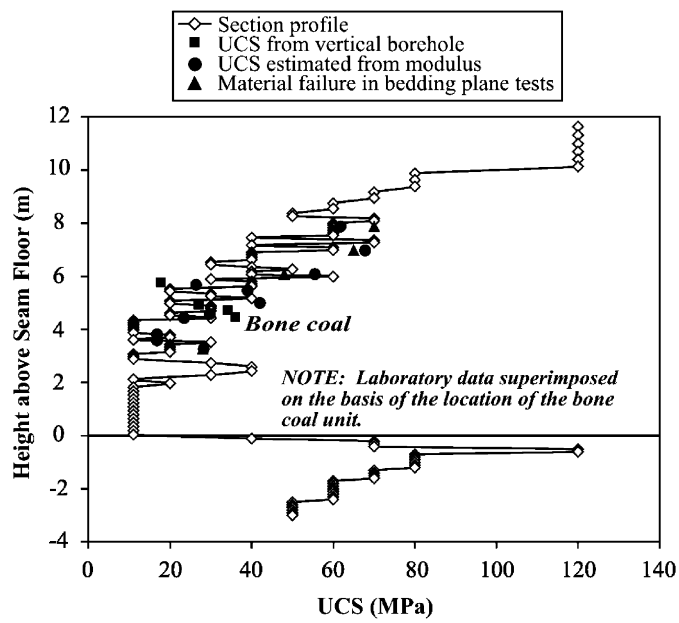

Fig. 6. UCS profile used in the model together with rock property data derived from testing.

[1]The multi-stage triaxial test aims to define the rock strength envelope for a number of confining pressures (2, 5, and 10 MPa) using a single sample. A stiff, servo controlled testing machine must be used in the deformation control mode. The sample is loaded progressively until the onset of initial fracture, and then the confining pressure is increased to the next stage and the test continues. At 10 MPa confining pressure the sample is taken to full failure and then the confining pressure is released slowly and the residual strength monitored to determine the post failure strength envelope. When angled core samples are tested, the failure takes place along a bedding plane, and the applied stresses are resolved into the shear and normal stresses as shown in Fig. 3. An early application of multi-stage triaxial testing is described in Dolinar et al. [13].

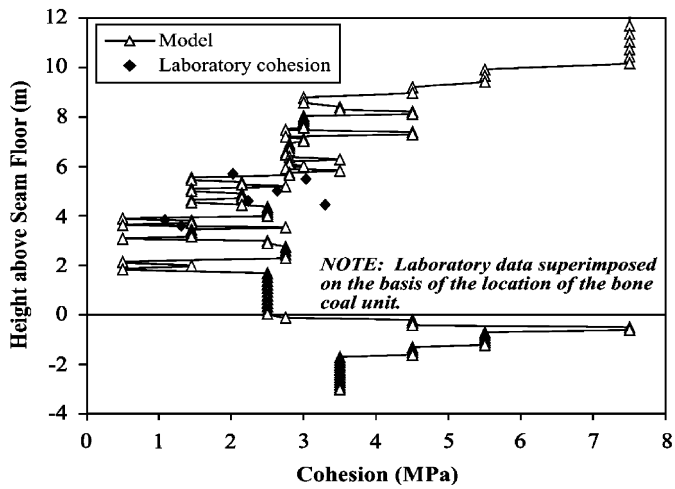

Fig. 7. Bedding plane cohesion profile used in the model together with rock property data.

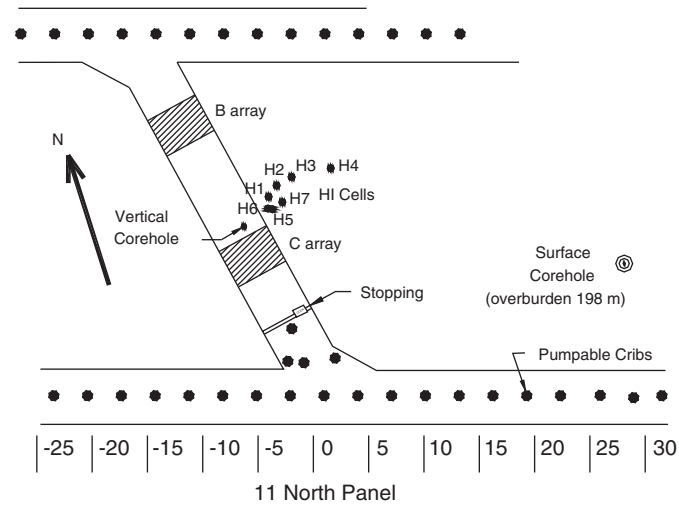

Fig. 8. Site map. Distances shown are meters from the center of the crosscut.

respectively. The layer-to-layer variations in the model profiles were derived from both the test results and inspection of the roof core. The in situ strength of coal within the model was set at 6.5 MPa (900 psi), which is typical of the bulk strength of coal.

The stress field has been measured in several locations in the Emerald and the adjacent Cumberland mine, but not at the specific study site. These measurements were reviewed to assess the range of stresses anticipated at the test site. The major stress was oriented N70°E. The regional stress field appears to be relatively consistent with a lateral tectonic strain [14] of approximately 550 microstrain. This means that the maximum stress is inferred to be approximately 11 MPa (1600 psi) for a rock having a Young's Modulus of 20 GPa (3 million psi). The horizontal stress within other rock units will be different and dependent on their elastic properties. The minor horizontal stress is estimated to be approximately half of the major stress. Vertical stress is approximately 5 MPa (700 psi) and related to overburden of approximately 200 m (650 ft).

Primary roof support used in the area of this study consisted of three 22 mm ($\frac{7}{8}$ in) diameter, 2.4 m (8 ft) long combination bolts. The bolts were installed with 1.2 m (4 ft) resin cartridges in 35 mm (1–$\frac{3}{8}$ in) boreholes. The yield load of the bolts was 19 ton (21 ton) with an ultimate capacity of 28 ton (31 ton). At one of the instrumentation arrays, supplemental support consisting of rows of three cable bolts were installed between the rows of primary bolts. The cable bolts were 3.6 m (12 ft) long, 15 mm (0.6 in) diameter, and they were partially grouted with 1.2 m (4 ft) of resin.

3. Field instrumentation

At the site, two monitoring arrays were installed in a crosscut and a third in the adjacent tailgate entry (Fig. 8). The two crosscut sites, labeled sites B and C, are the focus of this paper. Conditions in these sites were more severe than in the tailgate site because the crosscut was oriented less favorably relative to the regional maximum horizontal stress.

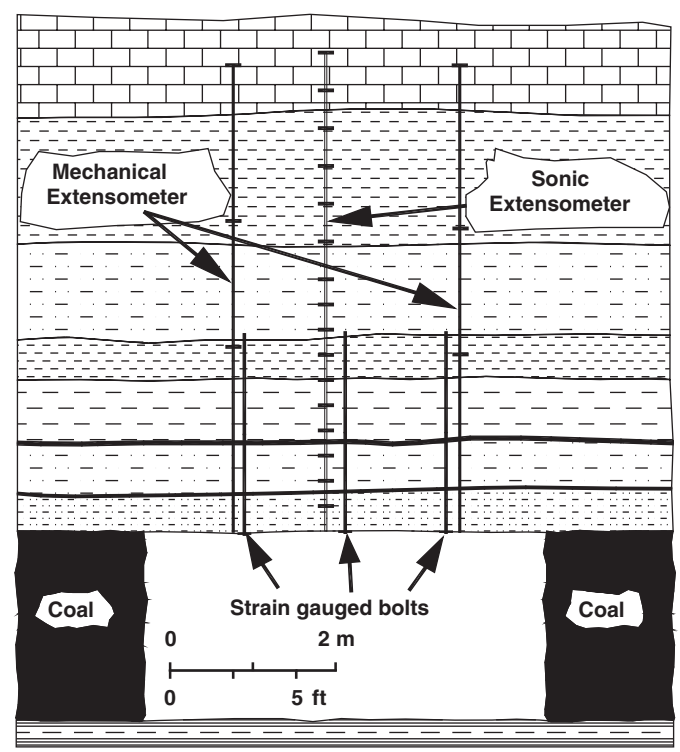

Fig. 9. Typical instrument array. The C site included nine rows of three cable bolts, and one row instrumented with U-cells in addition to the instruments shown.

Instruments were deployed to measure roof movements, support loads, and roof stress changes. Fig. 9 is a cross section showing the instrumentation in each array. The most detailed roof movement data were provided by multi-point sonic extensometers, with magnetic anchors located approximately every 0.3 m (1 ft) to a height of 5.8 m (19 ft) above the roof line. These were supplemented by

mechanical, three point extensometers that were monitored remotely.

Loads on the lower, 1.2 m (4 ft) long ungrouted portions of the combination roof bolts were measured using strain gauges installed inside the bolts using the technique developed by Dr. Hani Mitri at McGill University [15]. The instrumented bolts were obtained from Emerald Mine and prepared at McGill. Holes were drilled into the head of each bolt to accept a single strain gauge, near the bolt head, and electrical connectors. The bolts were individually calibrated to 13 ton (14 ton) by NIOSH and found to have a highly linear load-to-strain-gauge-signal response in the elastic range. NIOSH also tested combination bolts to determine the post-yield load-deformation relationship, so that estimates could be made of the bolt loads beyond yield. During the study the strain gauged bolts performed well, with no failures. Hydraulic U-cells were used to monitor the loads on three cable bolts at site C, but unfortunately only one provided useful measurements.

Horizontal stress changes were measured by seven CSIRO hollow inclusion (HI) cells that were installed in the roof above the gateroad pillar inby the crosscut site. Each HI cell consisted of an array of 12 strain gauges arranged to allow three-dimensional determination of stress changes. The cells were grouted in place using an epoxy designed specifically for HI cells to provide coupling between the rock and the gauges in the cell. Seven cells were installed with a 100% success rate using procedures developed by Dr. Jan Nemcik of SCT. Before installation, the holes were undercored to identify appropriate setting zones and to obtain samples for physical property testing.

The stress cells were installed in a fan pattern as shown in Fig. 10. Cell H7 was installed towards the top of the lower shale unit, while cell H6 was placed in the bottom of the limestone. The other five cells were installed to provide information on the stress distribution within the upper claystone unit. The strain data obtained from the HI cells were reduced using software developed by the US Bureau of Mines [16]. For presentation purposes, the stress changes have been transformed into principal stresses perpendicular to the crosscut.

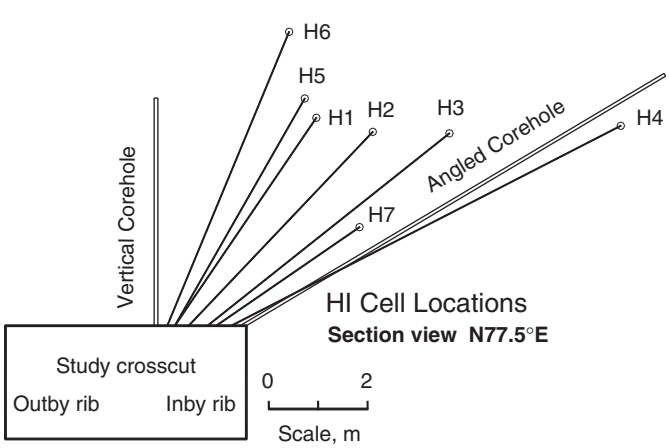

Fig. 10. Section view of HI cell locations.

4. Modeling approach and model used

Detailed monitoring studies conducted in coal mines in a number of countries have shown that the mechanisms of failure about excavations can be highly complex, involving fracture of rock, failure of bedding or joints, buckling of parted rock, and slip along weak surfaces [1,4,9]. The use of computer simulation therefore requires a detailed geotechnical characterization of the strata and stressfield, and must incorporate the many potential failure mechanisms [17,18]. Generalization of the rock properties or the rock mass section on the basis of averaged properties has been found to limit the capability to reproduce actual rock mass behavior.

The code used in the model is FLAC which has been modified to employ rock failure routines developed by SCT Operations. The constitutive models used by SCT are very similar to the strain-softening, ubiquitous joint model (SU) included with the latest release of FLAC2D [19]. Rock failure is based on Mohr–Coulomb criteria relevant to the confining conditions within the ground. A broad range of potential failure modes are simulated including:

- shear fracture of intact rock;
- tension fracture of the rock;
- bedding plane shear; and
- tension fracture of bedding (bedding separation).

The stability of pre-existing jointing, faults or cleat is also addressed in the simulations where appropriate. The model simulates new or re-activated rock fracture and stores the orientation of the fractures.

In the SCT constitutive model, as well as Itasca's SU, the intact rock matrix exhibits strain-softening post-failure behavior. A weakness plane of any orientation is also included in the model, and this weakness plane can also exhibit strain-softening behavior. This constitutive model is most appropriate for coal measure rocks where the intact rock is strain-softening and one dominant weakness plane exists, namely horizontal bedding. In both SCT's and Itasca's constitutive models, cohesion, friction angle, dilation angle and tensile strength are specified as functions of the "plastic strain." Depending on the nature of these functions, a variety of complex hardening and softening behaviors can be produced.

The in situ strength of the rock materials is reduced to 0.58 of the laboratory unconfined compressive strength (UCS). This lab-to-field scaling factor was originally was suggested by [20], and is routinely used in all SCT model studies.

The model geometry is presented in Fig. 11 with the various rock layers characterized by their laboratory UCS. The typical element size in the region of interest is approximately 20×10 cm (8×4 in). This element size is

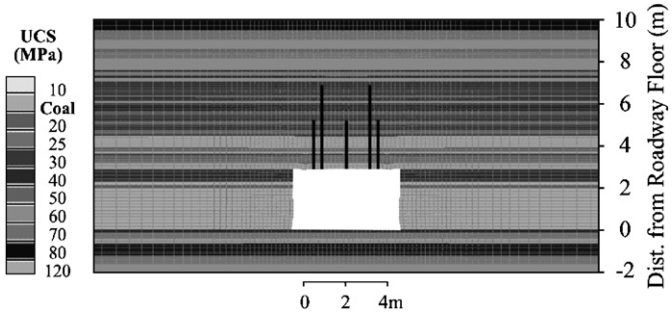

Fig. 11. Model geometry and UCS of rock units.

fine enough to capture geologic variations that may be important at the coal mine entry scale.

Rock bolts were included in the model. The bolts were bonded in the upper 1.2 m with a free length to the roof line. Yield of bolts was 19 ton (21 ton) with a pullout force of approximately 15 ton/ft. Cable bolts were also modeled as partially bonded with a yield capacity of 25 ton (27 ton). Care was taken to simulate the shear strength and stiffness properties of the resin/rock interfaces of the bolts. All of the bolt properties were adjusted to account for the row spacing in the 2-D model.

The modeling sequence followed the actual entry development process in that the entry was first excavated, then the outside roof bolts were installed, and finally the center bolt was installed. The model was allowed to respond to each of these steps. If cable bolts were used in a model, they were placed last.

For this model, a plane of symmetry was used at the roadway center line. The use of symmetry speeds the modeling process particularly in this case where a range of stress conditions or support systems is to be evaluated.

5. Results: field measurements

The study site was subjected to increasing horizontal stress during each of the three mining phases:

- the initial entry development;
- the start-up of the 10 North longwall; and
- the retreat of the 11 North longwall past the study site.

As the study site was developed, evidence of stress damage included a small "cutter" along the inby rib of the crosscut. Ground conditions at the study site notably deteriorated as the 10 North longwall began mining, even though the start-up room was located approximately 100 m (300 ft) away (Fig. 3). This was attributed to development of the horizontal stress concentration at the corner of the 10 North gob. Roof mapping conducted at the time showed that roof failure had extended some distance from the start-up room, and included at least one large roof fall. Apparently the breakup of the roof near the start up room caused a gradual transfer of stress to the vicinity of the study site.

The third phase, the approach and mine-by of the 11 North longwall, resulted in further roof deterioration associated with the stress concentration at the tailgate corner. Conditions were not as severe as had been encountered in past stress windows at the Emerald Mine, however, and the study site did remain accessible almost until the face passed.

Stress measurements: The HI cells were not installed until well after the entries were developed, so the stress changes associated with entry development were not recorded. Following the start-up of the 10 North longwall, the two HI cells that were in place showed roof stress increases on the order of 3.5 MPa (500 psi). The rate of stress increase gradually moderated, but never completely stabilized (see Fig. 12).

Fig. 13 is a snapshot of the stress changes that had been measured by the end of Phase 2 (startup of the 10 North longwall). The major principal stresses are all compressive, and range in magnitude up to 20 MPa (3000 psi). The orientations of the principal stress increases imply that the immediate roof of the crosscut yielded or "softened," and was not capable of transmitting additional horizontal stress. As a result, the stress was forced higher into the roof above the crosscut. The extensometer data that will be discussed later provides further evidence of the roof softening.

After the start-up of the 11 North longwall, definitive stress changes began to be observed in all HI cells when the face was approximately 192 m (640 ft) inby the center of the study tailgate intersection. After the face reached 27–32 m (90–110 ft) inby the cells the rate of stress change greatly accelerated. In most cases the stresses increased as the face approached, typically by about 7 MPa (1000 psi). The direction of the maximum principal stress increases continued to be in a generally sub-horizontal orientation, directed around the softened roof of the crosscut (Fig. 14). One notable exception was H7, installed in the lower shale unit, where the stresses remained almost constant as the face approached.

As the face passed by the site, nearly every HI cell measured an immediate horizontal stress reduction of about 10 MPa (1400 psi), indicating that caving of the immediate roof above the panel resulted in stress relief.

In summary, it appears that the mining-induced stress concentration approximately doubled the original in situ stress. The orientations of the stress increases measured by the HI-cells indicates that the stresses predominantly passed over, and not through, the softened (yielded) roof immediately above the crosscut.

Roof deformation: Initial extensometer readings were first made several days after development, so the data do not include the initial roof sag, but by mid-November the roof at all three sites had stabilized with less than 5 mm (0.2 in) total deformation (Fig. 15). However, the maximum height of roof movement was about 3.3 m (11 ft), well above the top of the bolting horizon at 2.4 m (8 ft).

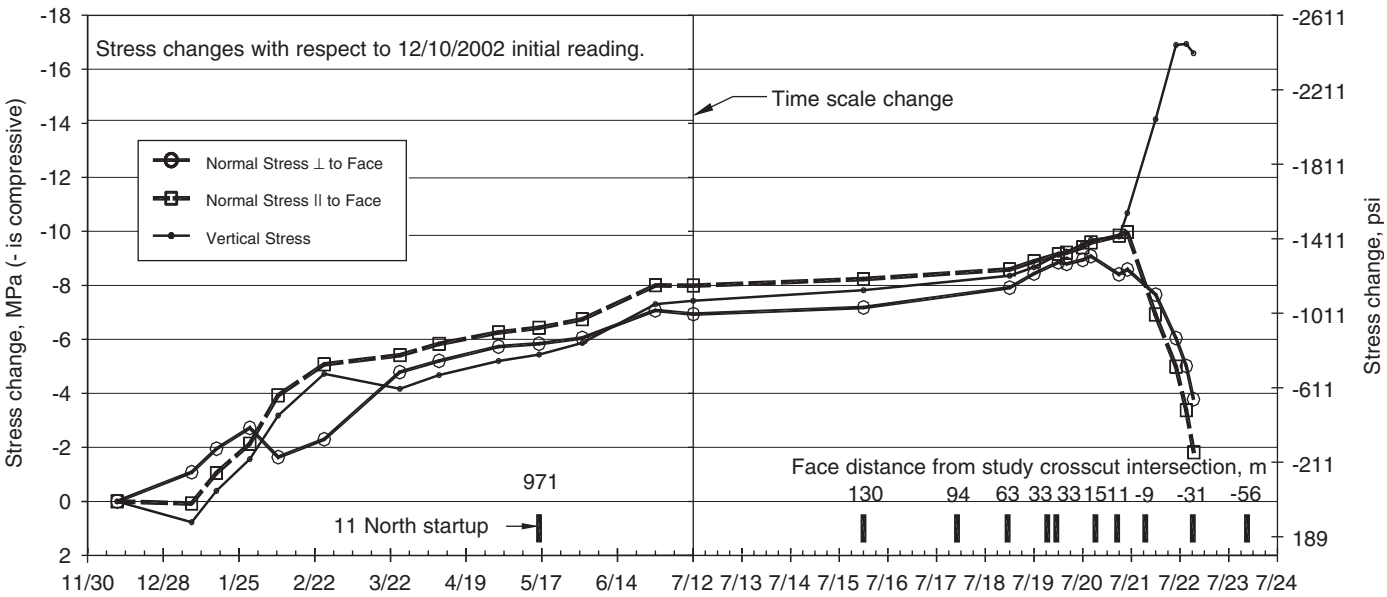

Fig. 12. HI cell stress changes from cell H4 located 4.0 m above the roof and 7.6 m into the gateroad pillar. Vertical and normal stresses parallel and perpendicular to the face are shown. The shear stresses are not shown. Negative values are compressive changes.

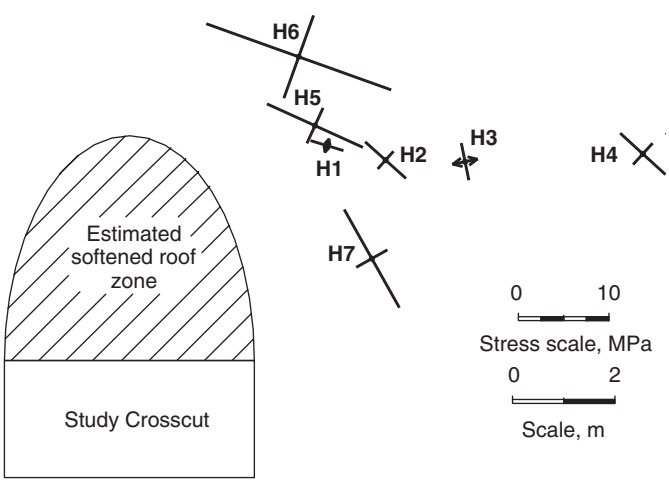

Fig. 13. Principal stress changes after the completion of the 10 North longwall and prior to mining the 11 North longwall in the plane perpendicular to the study crosscut, with respect to initial HI cell readings. Stress changes with arrows are tensile or stress relief; stress changes without arrows are compressive.

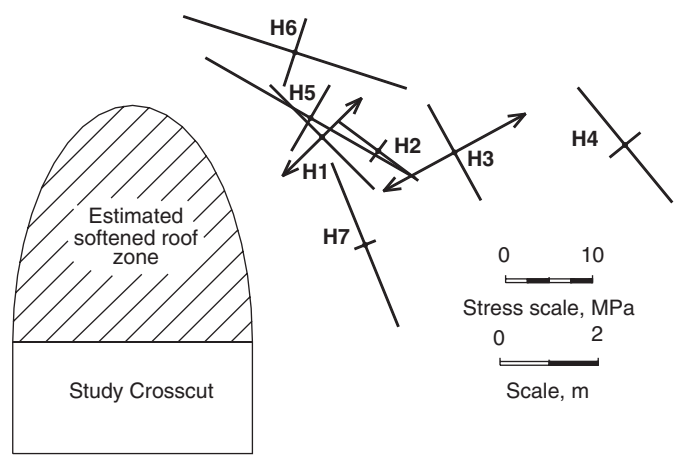

Fig. 14. Principal stress changes through 0330 on July 21, 2003 in the plane perpendicular to the study crosscut, with respect to initial HI cell readings. The face is 2 m (8 ft) outby the study crosscut tailgate entry intersection. Stress changes with arrows are tensile or stress relief; stress changes without arrows are compressive.

During Phase 2, the 10 North start-up period, the maximum height of roof deformation at the B and C arrays increased to 3.9–4.2 m (13–14 ft.), with total deformations of 16 and 10 mm (0.6 and 0.4 in), respectively (Fig. 15). Further evidence of roof softening during this period is apparent in the measurements of bolt loads and roof movements. Maximum roof strains in excess of 1.5% were measured at two points in the B extensometer, while the C extensometer had one location where the strain exceeded 1%.

As the 11 North face approached, both of the sonic extensometers in the crosscut recorded significant roof movements. Total deformations in each increased by about 20 mm (0.8 in) and the height of roof movement reached 4.9 m (16 ft). Most of this deformation occurred during the last 23 m (75 ft) of advance before the face reached the crosscut.

While the two arrays differed in the timing and magnitude of the roof deformation, it was significant that the deformation process followed a broadly similar pattern in both locations. The maximum height of movement was approximately 5 m (16 ft), and significant roof strains occurred both near the top of the combination bolts (at 2.4 m) and approximately 1.5 m (5 ft) above them.

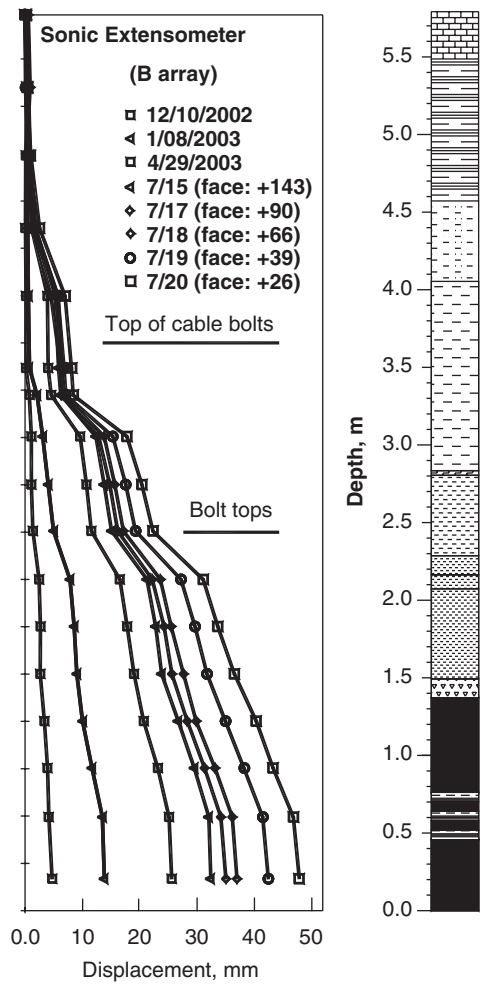

Fig. 15. Profile of roof movement in the study crosscut at the B array sonic extensometer, from December 2002 through the last reading on July 20, 2003, with roof lithology. Face distances shown are in meters, with the face in by the extensometers. Depths are referenced to the roof line.

Roof bolt loads: Fig. 16 shows the average bolt loads that were measured during the course of the study at the two instrument arrays. When they were first installed, the initial roof bolt loads were typically 3–8 tonnes. During the next several weeks the loads increased, particularly at the B-site, the site without cable bolts. In fact, Fig. 16 shows that while the initial loads were higher at the C-array, the loads on the B-array bolts soon exceeded those on the C-bolts and then remained higher throughout the course of the study. The lower loads on the C-bolts were attributed to the presence of the supplementary cable bolts (although the ventilation stopping near the C array may also have provided some support [21]).

With the start-up of the 10-North longwall, the loads on the B-array bolts increased another 3–5 to 12–22 tonnes, with the highest readings indicating that bolts were reaching yield. At the C array bolt load increases were somewhat less, to 8–15 ton.

By the time the 11 North face was within 40 m (130 ft) of the site, all of the B-array bolts were in yield. One C array bolt went into yield suddenly when the face was 105 m (340 ft) inby, and the center bolt yielded almost as the face passed. The cable bolts reached their maximum recorded loads at this time, apparently below yield. After the face passed the study crosscut the mechanical extensometers indicated that roof deformations large enough to load a cable bolt well into yield (more than 50 mm) took place below the tops of the cable bolts. Bolt loads at the crosscut arrays reached a maximum shortly after the face had passed, and then began to decrease.

Unfortunately, the loading record for the cable bolts was incomplete due to instrument problems. However, the nearly 50 mm (2 in) of measured roof movement, along with the lower bolt loads measured at array C, both support the indication from the measurements that are

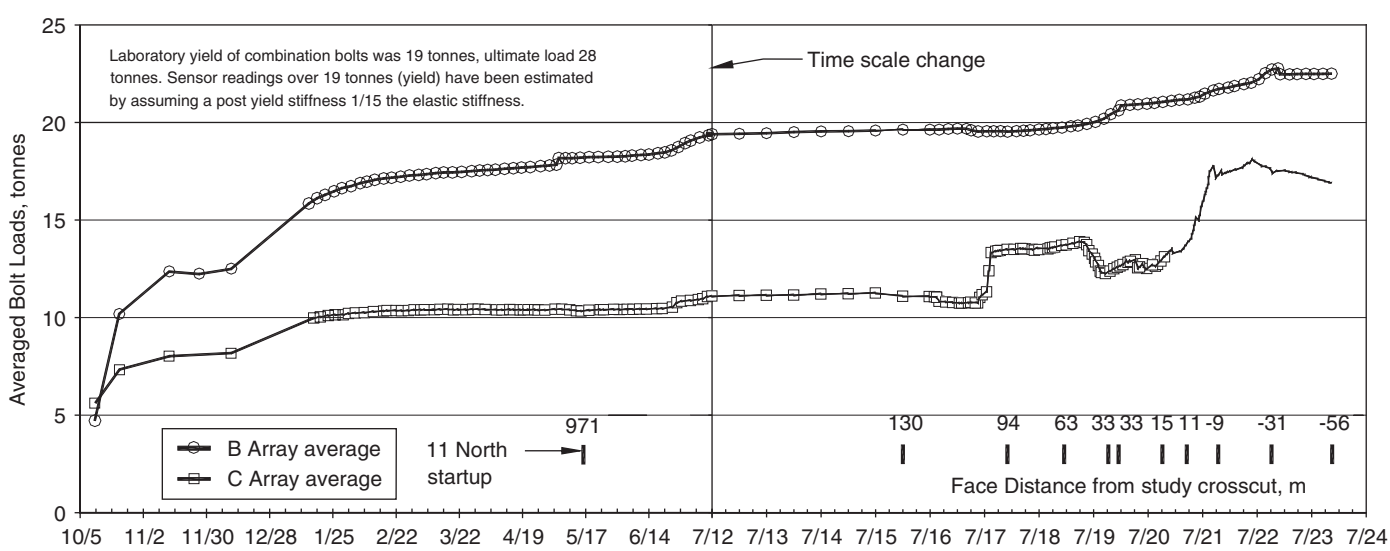

Fig. 16. Bolt loads. Strain gauged bolts only, from the B and C arrays. Each curve is averaged from three bolts.

available that the cables did assume a significant portion of the roof load. Recent field and numerical model studies [6,22] both indicate that supplemental supports probably reduced the loads that would have otherwise have been applied to the roof bolts.

6. Stress path used in the model

The far-field (boundary condition) horizontal and vertical stresses applied to the model at each successive stage of the modeling process is the "stress path." The stress path represents the incrementally increasing stresses that developed during the initial development of the study crosscut and the subsequent extraction of the two longwall panels. The stress path employed in this study is presented in Fig. 17. It was estimated from the anticipated in situ stresses, the stress change measurements made at the site, and measurements made at similar sites in past studies. Another indication of the "far field" stress increase associated with longwall mining at this site was the approximately 10 MPa (1400 psi) of stress relief that was measured following the passage of the longwall face.

7. Modeling results: roof movement

The comparison between the model results and the field measurements relies heavily on the roof extensometer data. The approach has been to compare the extensometer results at approximately equivalent total displacements at the roof line. In this way, the nature and style of deformation within the roof which causes the total displacement can be compared. This allows the performance of different support systems to be evaluated using the same criteria that are employed in the mine—namely, how much roof movement is taking place. Therefore, it is not necessary to employ surrogates such as the maximum stress or a safety factor.

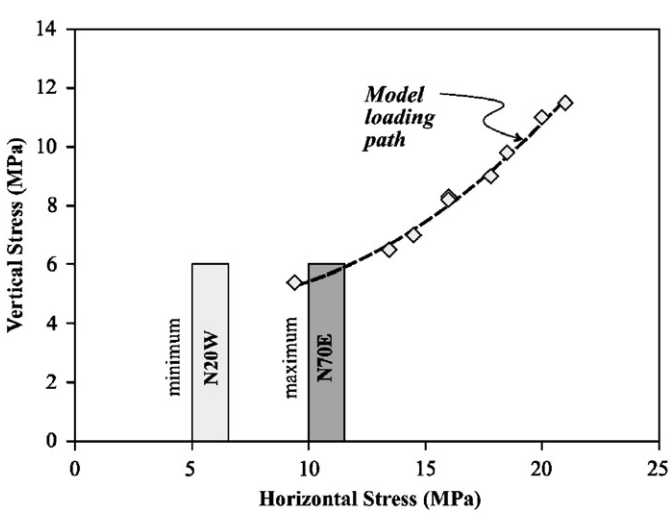

Fig. 17. Stress path modeled representing increasing stress during development and longwall extraction operations.

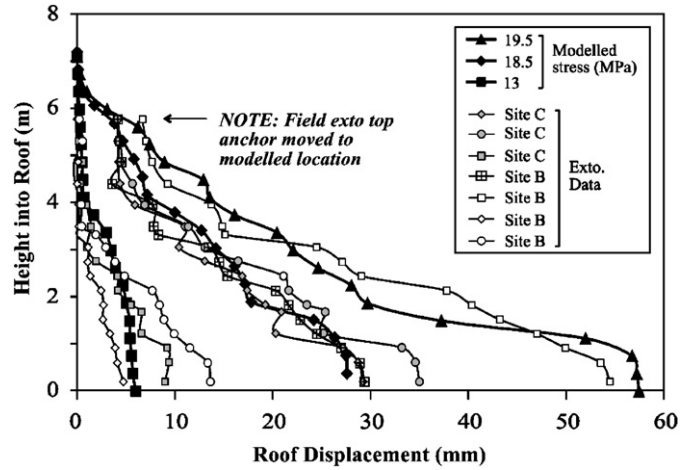

Fig. 18. Comparison of modeled and measured roof displacement profiles.

Fig. 18 compares the roof deformations calculated in the model to those measured underground. Model results from three stress levels on the model loading path are shown. Also shown are a number of deformation profiles measured at the two crosscut sites. The figure indicates that the model was able to capture the deformation pattern common to both sites, showing a very close correlation in both deformation style and height of movement. It should also be noted that the model indicated that some deformation occurred even above the top of the extensometers.

Fig. 19 illustrates the location and nature of the rock failure processes that are associated with the roof deformation profiles. Upon initial development (Fig. 19a) bedding plane shear occurs readily within the section and early in the deformation process. As stress levels increase shear fracture of the weaker shale units occurs. Higher stress levels cause shear of the stronger materials together with additional bedding plane shear. However, total roof deformations are relatively minor until the applied far-field stress reaches approximately 15–16 MPa (2200 psi; Fig. 19b). Beyond that stress level, significant roof deformation develops and progresses higher into the roof section (Fig. 19c).

8. Modeling results: roof bolt forces

The roof bolt forces developed in the model and roof bolt load data from sites B and C are presented in Fig. 20. To make the comparison, the average bolt loads were determined for three levels of roof displacement. In general, there is a fairly wide range in average bolt load at the monitoring sites, however, the overall forces developed in the model are consistent with the range as monitored. This provides an indication that the bolt-strata interaction is being simulated in a realistic manner consistent with the site response.

The results indicate that under the in situ development stress state (less than approximately 11–12 MPa (1600 psi))

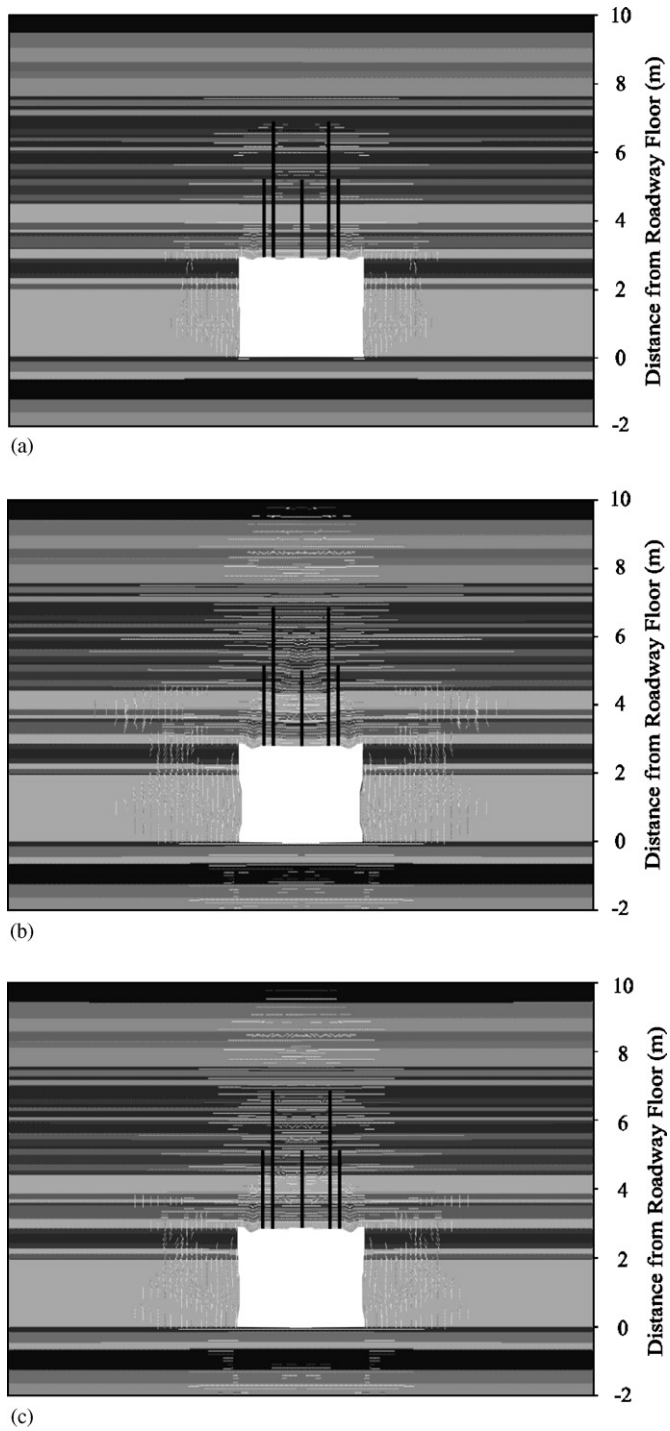

Fig. 19. Roof deformation in the model at three stress levels: (a) 11–12 MPa, (b) 16 MPa and (c) 19 MPa.

roof conditions would be anticipated to be good and well controlled by the bolt pattern placed. The roof bolts continue to be well under yield load up to a stress level of approximately 15–16 MPa (2200 psi). Once significant roof deformations begin to occur, however, the bolt loads rapidly increase.

The model results (Fig. 20) show that the addition of cable bolts initially has little effect on bolt loads. However,

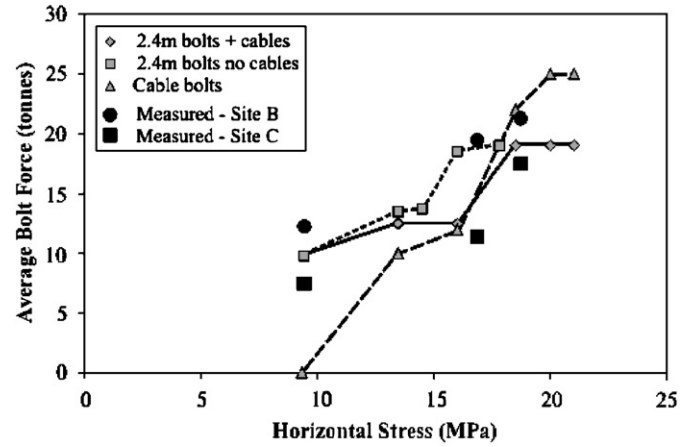

Fig. 20. Roof bolt forces developed relative to horizontal stress.

once major roof movements begin to occur, the cables assume enough load to delay the onset of yield in the roof bolts. The cable bolts appear to develop their full capacity after the roof bolts yield.

9. Modeling results: stress redistribution about the cross cut caused by roadway deformation

The measurements made during the study showed that the additional stresses were redirected above the immediate roof of the crosscut even before significant roof deformations had occurred (Fig. 13). The model indicated that the bedding plane shear that developed early in the deformation process could be sufficient to cause significant stress redirection even though the displacement and visual deformation of the roadway was low. An example is presented in Fig. 21 for an equivalent displacement of approximately 20 mm (8 in).

The amount of horizontal stress transferred within the initial 2 m (7 ft) of roof at the center of the roadway is an indication of the stability of the roof section and the requirement for reinforcement of the rock. When the bolted roof section has lost its integrity and become "softened," the horizontal stress it can carry is reduced. Once extensive rock fracturing causes roof softening, the reinforcing action of the reinforcement is the primary design task.

In summary, it appears that the model results are consistent with the monitored and observed behavior of the roadway available at the site. This provides confidence that the model is simulating the rock deformation processes influencing roadway stability and reinforcement interaction. This confidence allows for realistic assessment of various bolt patterns within the stress conditions anticipated at the site, as discussed in the next section.

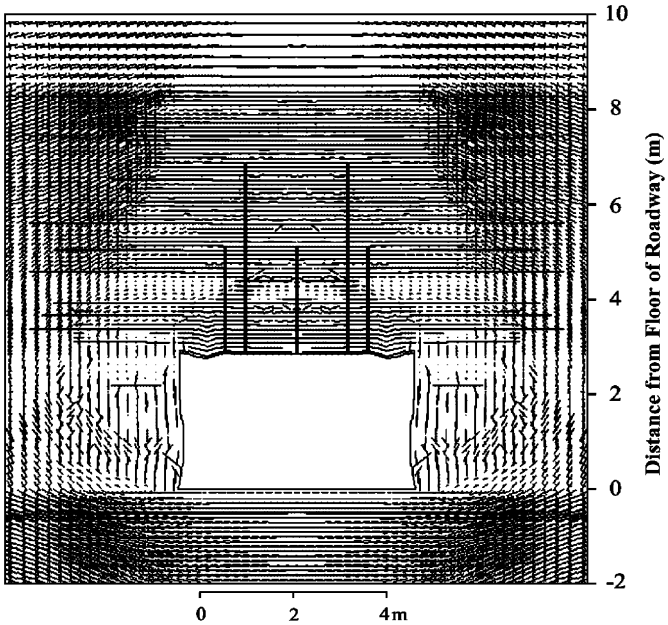

Fig. 21. Stress redirection about the roadway caused by localized rock failure and subsequent changes in bulk material properties during roadway development.

10. Application of the modeling results to reinforcement design

In this section, the effect of hypothetical bolt patterns were evaluated to demonstrate the influence of reinforcement patterns on roadway behavior.

The bolt patterns assessed in this example were:

1. 3, 1.8 m (6 ft), long fully grouted bolts.
2. 3, 2.4 m (8 ft), long combination bolts.
3. 3, 2.4 m (8 ft), long combination bolts with 2, 4 m (13 ft) cables.

Fig. 22 shows the roof displacement within the roof section. Each bolt system has a characteristic "limit" at which point the roof deformations begin to rapidly increase. It is significant that the deformation does not follow a smooth curve towards failure, but rather abruptly goes from "controlled" to "uncontrolled" movement. This seems to conform with underground experience, where "good" conditions often seem to "suddenly" go bad.

For the standard 2.4 m (8 ft) bolt pattern, the roof maintains integrity up to approximately 15–16 MPa (2200 psi), which is within the range anticipated during development at high angles to the regional stress field. The addition of supplemental cable bolts would allow the roof to cope with an additional 3–4 MPa (500 psi).

On the other hand, 1.8 m (6 ft) bolts reach their limit at just 12 MPa (1700 psi), which could change a situation of probable roof control success during development in the cross cut direction to one of potentially difficult roof conditions. These results are consistent with expectations,

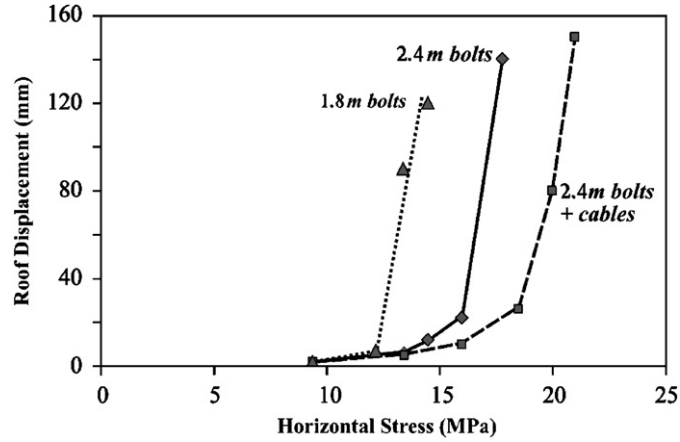

Fig. 22. Displacement of the roof section for various bolt patterns.

and indicate that various combinations of reinforcement can significantly modify the deformation limit of the strata section.

11. Conclusions

The study confirmed that the "stress window" that resulted from the mining geometry did cause a dramatic increase in the horizontal stress at the site. The measurements indicated that the stress approximately doubled as the mining progressed.

In the vicinity of the entry, these stresses were significantly reoriented by the deformation and failure that developed in the mine roof. The zone of measured "roof softening" extended above the height of the bolts, causing the additional horizontal stress to be transferred higher into the roof. The softened zone did not become a fully "detached block", however. Even site B, which was supported by just the normal roof bolt pattern, did not collapse. However, the roof bolts at site B did yield much earlier in the study than did those at site C, where supplemental cable bolts had been installed. It appeared that the cable bolts assumed a portion of the loads that would otherwise have been applied to the roof bolts.

The numerical model was able to capture the most significant aspects of the behavior of the study site. The modeled roof deformations matched the measured ones in both magnitude and location. A critical element in the model's success was its ability to simulate the extensive bedding plane slip that developed in the roof.

Additional modeling showed that each support pattern had a critical level of applied horizontal stress beyond which roadway conditions dramatically deteriorated. For example, 1.8 m (6 ft) bolts perform adequately up to an applied stress level of approximately 12 MPa (1700 psi), and increasing the length of the roof bolts to 2.4 m (8 ft) allows the entry to survive stresses up to 15–16 MPa (2200 psi). Adding cable bolts would increase the capacity of the support system by approximately another 20–25%. It seems, therefore, that the model could be used to select

the optimum support pattern if the expected stress increase could be estimated.

References

[1] Mark C. Design of roof bolt systems. New technology for coal mine roof support, proceedings. NIOSH open industry briefing, NIOSH IC 9453, 2000. p. 111–31.

[2] Gale W, Nemcik JA, Upfold, RW. Application of stress control methods to underground coal mine design in high lateral stress fields. In: Proceedings, sixth international congress on rock mechanics. International Society for Rock Mechanics; 1987. p. 897–900.

[3] Mark C. Horizontal stress and its effects on longwall ground control. Mining Eng 1991:1356–60.

[4] Gale WJ, Fabjanczyk MW, Tarrant GC, Guy RJ. Optimization of reinforcement design of coal mine roadways. In: Proceedings, 11th international conference on ground control in mining, Wollongong, NSW, Australia, 1992. p. 272–9.

[5] Mark C, Mucho TP, Dolinar DR. Horizontal stress and longwall headgate ground control. Mining Eng 1998:61–8.

[6] Tadolini SC, Barczak TM, Zhang Y. The effect of standing support stiffness on primary and secondary bolting systems. In: Proceedings, 22nd international conference on ground control in mining, Morgantown, WV, 2003. p. 300–9.

[7] Mark C, Dolinar DR, Mucho TP. Summary of field measurements of roof bolt performance. New technology for coal mine roof support. In: Proceedings, NIOSH open industry briefing, NIOSH IC 9453. 2000. p. 81–98.

[8] Signer S. Load behavior of grouted bolts in sedimentary rock. New technology for coal mine roof support. In: Proceedings of the NIOSH open industry briefing, NIOSH IC 9453. 2000. p. 73–80.

[9] Gale WJ, Fabjanczyk MW. Design approach to assess coal mine roadway stability and support requirements. In: Proceedings, eighth Australian tunnelling conference, Sydney, 1993.

[10] Hayes AW, Altounyan PFR. Strata control: the state-of-the-art. Mining Technol IMM 1995;77(892):354–8.

[11] Gale WJ, Tarrant GC. Let the rocks tell us. In: Proceedings, symposium on safety in mines, the role of geology, 24–25 November 1997. p. 153–60.

[12] Mark C, Molinda GM, Barton TM. New developments with the coal mine roof rating. In: Proceedings, 21st international conference on ground control in mining, Morgantown, WV, 2002. p. 294–301.

[13] Dolinar DR, Horino FG, Hooker VE. Mechanical properties of oil shale and overlying strata, naval oil shale reserve. Anvil Points, CO: US Bureau of Mines RI 8608; 1982 (43p).

[14] Dolinar DR. Variation of horizontal stresses and strains in mines in bedded deposits in the eastern and midwestern United States. In: Proceedings, 22nd international conference on ground control in mining, Morgantown, WV, 2003. p. 178–85.

[15] Mitri H, Marwan J. A new rockbolt axial load measuring device. In: Proceedings, 20th international conference on ground control in mining, Morgantown, WV, 2001. p. 367–73.

[16] Larson M. Stressout—a data reduction program for inferring stress state of rock having isotropic material properties: a user's manual. US: US Department of the Interior, Bureau of Mines IC 9302; 1992 (163p).

[17] Gale WJ. Experience in computer simulation of caving, rock fracture and fluid flow in longwall panels. In: Proceedings, international conference on geomechanics/ground control in mining and underground construction, vol. 2, Wollongong, NSW, Australia, 14–17 July 1998. p. 997–1007.

[18] Kelly M, Gale WJ, Luo X, Hatherly P, Balusu R, LeBlanc G. Longwall caving process in different geological environments better understanding through the combination of modern assessment methods. In: Proceedings, international conference on geomechanics/ground control in mining and underground construction, vol. 2, Wollongong, NSW, Australia, 14–17 July 1998. p. 573–89.

[19] HCItasca, FLAC 4.0 users guide. 2000.

[20] Hoek E. Brown, ET, underground excavations in rock. London: IMM; 1980 (527p).

[21] Oyler DC, Hasenfus G, Molinda GM. Load and deflection response of ventilation stoppings to longwall abutment loading—a case study. In: Proceedings, 20th international conference on ground control in mining, Morgantown, WV, 2001. p. 34–41.

[22] Barczak TM, Chen J, Bower J. Pumpable roof supports: developing design criteria by measurement of the ground reaction curve. In: Proceedings, 22nd international conference on ground control in mining, Morgantown, WV, 2003. p. 283–93.